Frontiers in Mechanochemistry and Mechanical Alloying

INCOME2008
1-4 December, 2008

EVALUATION OF INTERFACE MICROSTRUCTURE FOR FRICTION STIR WELDED ALUMINIUM-STAINLESS STEEL PLATE

M. Ghosh[1ξ], A. Kar[3], K. Kumar[2], S. V. Kailas[2], S. K. Das[1], A. K. Ray[1]
[1]Materials Science and Technology Division, National Metallurgical Laboratory (CSIR), Jamshedpur – 831007, India
[2]Department of Mechanical Engineering, Indian Institute of Science, Bangalore – 560012, India
[3]School of Advanced Materials Science and Engineering, Sungkyunkwan University, South Korea-440-746

Keywords: Friction stir welding, Aluminium, Stainless steel, Analytical electron microscopy, Tensile strength.

Abstract

In the present study, commercially pure aluminium has been joined with 304 stainless steel by friction stir welding. Microstructural characterization was carried out using scanning and transmission electron microscopes. Diffusion of Fe, Cr and Ni is substantial within Al; however diffusion of Al within 304SS is limited. Owing to inter-diffusion of chemical species across the bond line, discrete islands of Fe_3Al intermetallic phase forms within the reaction zone. The rubbing action of tool over the butting edge of 304SS removed fine particles of 304SS and got embedded in the stirring zone of Al matrix. At the latter stage austenite underwent phase transformation to ferrite due to large strain within its grain. Fracture path mainly moves through stirring zone of Al alloy under tensile loading; however in some places, presence of Fe_3Al compound has been found.

Introduction

Friction stir welding (FSW) is obtained by inserting a spinning tool pin into the surface of adjoining metal sheet edges [1]. The extent of asymmetric material flow during the process with respect to the pin axis principally governed by pressure, temperature and generated strain which, in turn depend on tool rotational speed, feed rate and the normal load on the job [2-3]. The asymmetry develops advancing and retreating side along the bondline. The process is widely investigated for low melting materials like Al, Cu and Mg [4-10]. Difficulties arise at the time of joining high temperature alloys like steel as the temperature rise during processing is quiet high and it is not easy to get suitable tool material. However, W-Re alloys and poly crystalline cubic boron nitride have been used to weld variety of steels [11-17]. The Problems become severe, when FSW is carried out for dissimilar material combination having wide differences in melting points and deformation characteristics. Still, to cater complex function by a single component and to reduce the fabrication cost, joining of dissimilar material is inevitable. One example is joining of Al to ferrous alloys for automobile application with an aim to reduce fuel consumption. Arc and laser welding in that case develops brittle cast structure and intermetallics. Friction welding in this case is limited for joining other than sheet materials. The promising technique is friction stir welding and information related to the process for Al to stainless steel joining is limited. The objective of the present investigation is to study the microstructural changes i.e. occurring for the friction stir welded 304 stainless steel to commercially pure aluminium with an assessment of joint quality.

Experimental

Commercially pure aluminium (CP Al) and 304 stainless steel (304SS) plate having dimensions, 2.5 mm thickness x 60 mm width x 140 mm length were used for fabricating the joint. The chemical composition and mechanical properties of the alloys are furnished in Table 1 and 2, respectively.

Table 1. Chemical composition of the substrates in wt%

Element	Alloy Designation	
	CP Al	304SS
Al	Balance	-
Fe	0.1	Balance
Cr	-	18.2
Ni	-	8.41
Si	0.25	0.39
Mn	-	0.98
C	-	0.04
S	-	0.003
P	-	0.005
Others total	0.12	-

Table 2. Tensile properties of the alloys in as received condition at ambient temperature

Alloy designation	0.2% Off set yield (MPa)	UTS (MPa)	Breaking strain (%)
CP Al	35 ± 1	74 ± 2	41 ± 0.5
304SS	211 ± 2	520 ± 3	47 ± 1

Friction stir welding experiment was carried out at Indian Institute of Science, Bangalore in a heavy duty milling machine. 304SS plate was placed at the advancing side and the aluminium plate at retreating side. The welding tool assembly consists of die steel shoulder and tungsten carbide pin. The shoulder and pin diameter was 15 mm and 4 mm, respectively. During processing, the tool was plunged 100 % in the Al side and traverse slightly inclined to the 304SS-Al interface in such way the tool pin portion interfered 20 % into the 304SS at the end of 100 mm weld. The rotation speed, traverse speed and tool tilt angle were 1000 rpm, 50 mm/min and 2^o respectively. The normal load was 5 kN.

ξ email : mainakg@nmlindia.org

From the joint, sampling was carried out and metallographic specimen was prepared by conventional technique. The microstructure was observed in scanning electron microscope (JEOL JSM 840A) using energy dispersive spectroscope (Kavex). After locating the different zones, thin foils were prepared mechanically having thickness ≤0.09 mm. Then ultrasonic punching, dimpling and ion milling were done to obtain electron transparent area within a disc of 3 mm diameter. The foils were observed in analytical transmission electron microscope (CM200) operated at 200 kV. Tensile sample was prepared from transverse section of the assembly with the gauge length of 25 mm and tested at 0.1 $mm.min^{-1}$ cross head speed (Honsfield, H10K-S, 10 kN capacity). Fracture surfaces were observed in scanning electron microscopes (SEM) using energy dispersive spectroscope (EDS) to reveal the morphology and location of fracture.

Results

The SEM image of the assembly is shown in Fig.1. The bondline is visible. Three regions are resolved at higher magnification and the micrographs are furnished in Fig. 2 and Fig. 3. The bondline is irregular in nature as shown in Fig. 2(b). Dispersion of deeply shaded variable shape islands are found within the Al matrix in the stirring zone (SZ). Quantitative EDS analysis of that area (Fig. 4(c) indicates the concentration of chemical species as Al~0.70, Cr~18.0, Mn~1.4, Ni~9.6 and Fe (balance). This composition is more or less at par with the composition of parent 304SS. On bondline (Fig. 4(b)), the composition is Cr~4.0, Mn~0.9, Ni~8.3, Fe ~2.5 and Al (balance). Adjacent to bond line in 304SS side (Fig. 4(a)), Al concentration decreases (~5.4) at the expense of Fe (~65.9).

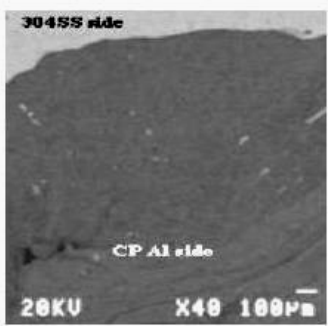

Figure.1. Low magnification SEM image of CP Al-304SS FSW assembly

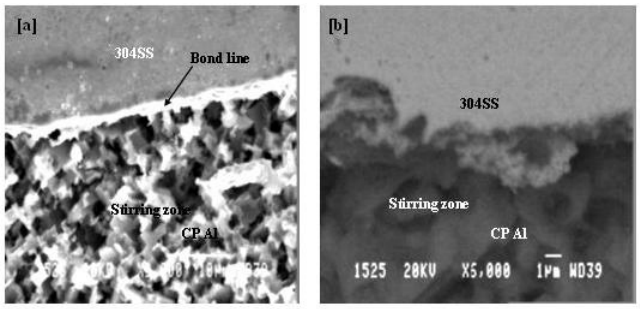

Figure.2. FSW joint between CP Al and 304SS near the stirring zone (a) SEM-SE and (b) SEM-BSE images

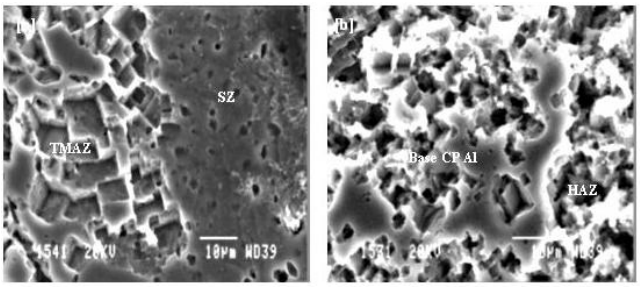

Figure.3. SEM-SE image of FSW joint between CP Al and 304SS (a) TMAZ-SZ and (b) HAZ-base CP Al

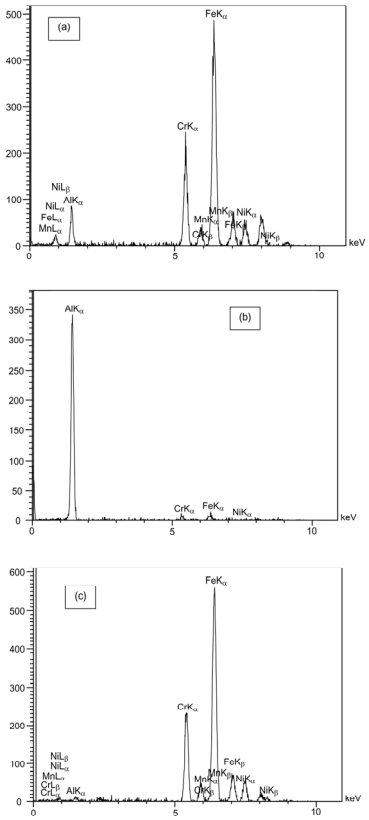

Figure 4. EDS analysis of FSW joint between CP Al and 304SS (a) on 304SS near bondline, (b) on the bondline and (c) deeply shaded phase in SZ of CP Al

Presence of Al within 304SS has not been detected beyond ~6µm whereas, in Al side qualitatively Fe, Cr, Ni has been found even at a distance of ~20 µm from bondline. It indicates limited diffusion of Al within the austenite matrix with no significant structural change.

Fig. 3(a) and 3(b) represent the photograph of thermo-mechanically affected zone (TMAZ) and heat affected zone (HAZ). Average grain size of TMAZ (~10-14 µm) is larger than the grain size of SZ (~ 8 µm). HAZ has practically negligible difference with the base CP Al (~22 µm).

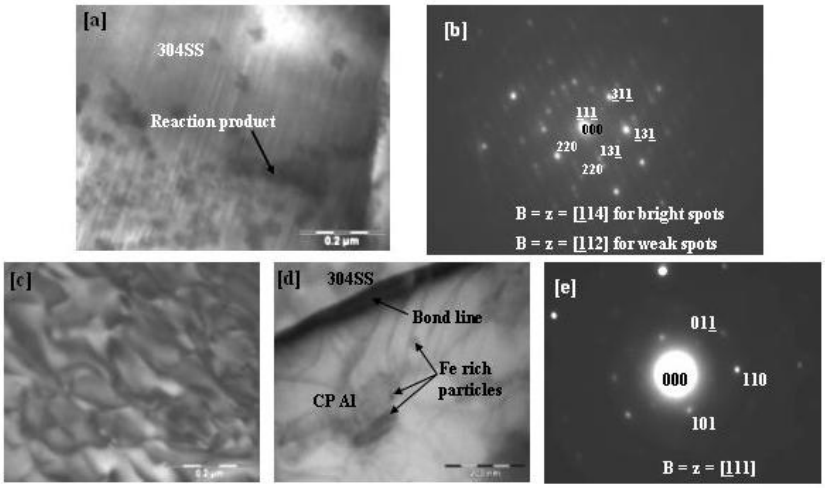

Figure 5. TEM micrographs of the SZ in CP Al side near the interface (a) islands of reaction product, (b) corresponding diffraction pattern of reaction product as shown in Fig.6 (a), (c) dislocation morphology in SZ, (d) Fe rich particles within the SZ of Al matrix and (e) corresponding SADP of Fe-rich particle

The microstructure of different zones in CP Al side was also observed in TEM to explore sub-micron detailings. The intermetallic phase appears as isolated island within the reaction layer (Fig. 5(a)) and the observation is at par with the Fig. 2(b) where, the irregularities have been also found. The corresponding indexed diffraction pattern confirms the presence of cubic Fe_3Al. The dislocation density within the stirring zone is high and leads to cell formation. The aspect ratio of the cell lies in the range of 1.5-2.3 (ratio of length to width). Dark areas within the matrix of aluminium exhibited variable shape and size (Fig. 5(d)). The diffraction pattern of that area (Fig. 5(e)) indicates the formation of ferrite.

TMAZ and HAZ does not exhibit any Fe-rich phase within the Al matrix. Dislocation cell formation is evident within the TMAZ having aspect ratio 1.5-3.4 (Fig. 6(b)).

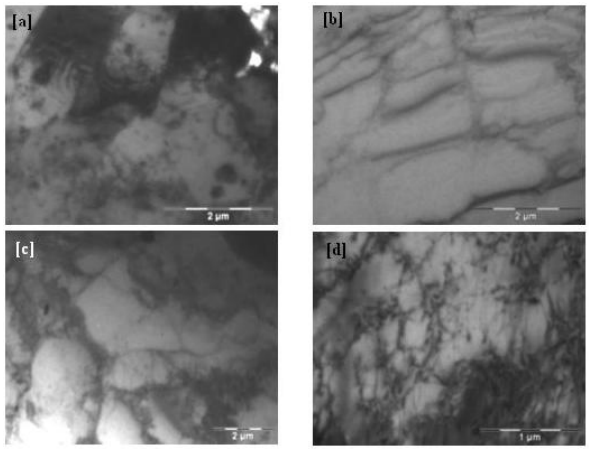

Figure 6. TEM micrographs of CP Al side (a) TMAZ (b) dislocation substructure in TMAZ. (c) HAZ and (d) base CP Al

HAZ and the base alloy does not exhibit much difference in microstructure; only in case of former qualitatively little higher dislocation density has been observed (Fig. 6).

The tensile property of the joint has been found to be 61±2 MPa with the breaking strain of 4.9±0.7%. The UTS value is thus 82% of that of parent aluminum. However, the ductility of the assembly is limited in comparison to the elongation of the substrate. Both the fracture surfaces of the assembly were observed in SEM (Fig. 7). The fracture surfaces exhibited the characteristics of micro-void coalescence. Quantitative EDS on fracture surface indicates besides aluminium, Fe concentration varies as 3.3-4.8wt% along with the presence of Cr.

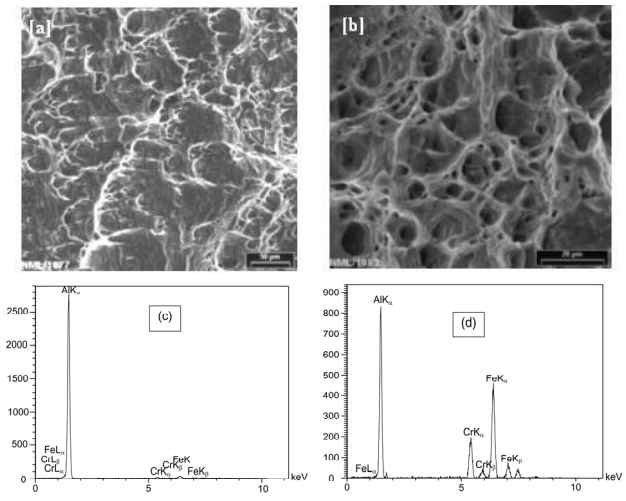

Figure 7. Fracture surface of FSW joint (a) CP Al side, (b) 304SS side, (c) bulk EDS on CP Al side and (d) bulk EDS on 304SS side

Discussion

In general, solid state welding occurs when a pair of contamination free metal surfaces is brought into the vicinity of inter-atomic-forces. Kumar et. al. have reported that, in FSW process the interface oxide layers on the faying surfaces are fragmented during severe plastic deformation and the fresh metal contact is established in the leading edge of the tool [18-19]. During traversing of the tool, a vertical contamination free surface is created in the advancing side due to an interaction of the tool with the material. Thus numerous fresh surfaces are created in the stirred zone due to material flow in friction stir welding and get consolidated in the trailing edge of the tool. A bond between the advancing side vertical interface and the stirring zone material is established by the forging of stirring zone material against the vertical interface. The frictional heat generation at the interface of the tool and base material is the reason for temperature rise in the weld region. Hence, the temperature rise in the interface during welding depends on coefficient of friction, rotation speed, traverse speed, contact load, hardness and thermal conductivity.

During processing of dissimilar alloys, the interface temperature is decided by the interaction volume of harder material. In FSW of 304SS, the temperature rise in the material is expected to be more than 1200 ^{o}C. For 304SS/Al dissimilar joints, if the FSW tool is plunged in middle of the interface, the temperature generated in the 304SS can melt the Al base material. To avoid the melting of Al, the tool has been plunged into the aluminium side and the tool interference with 304SS increased gradually during processing. The tool thus rubbed over the advancing side and de-touched particles are dispersed into the aluminium matrix, where stirring happens predominantly.

Diffusion of chemical species across the bondline is responsible for the change in microstructure. With respect to corresponding melting point of the alloy, the temperature rise in aluminum side is higher than the 304SS side. Hence, the diffusion of Fe, Cr and Ni within the aluminum matrix is higher than that of Al in austenite. This observation has been also illustrated by Yokoyama for friction welded 6061-T6 al alloy to 304SS [20]. Small transit time of the tool during processing hinders the creation of continuous layer of intermetallics; rather it appears as discrete islands within the reaction zone having width 40-60 nm. The composition of the intermetallic phase shows presence of Fe, Cr and Ni along with major quantity of Al. Hence, the intermetallic is cubic Fe_3Al in combination with Cr, Ni and Mn in solid solution. The presence of Fe_3Al has been confirmed by SADP (Fig. 5(b)). Moreover, as per the Fe-Al phase diagram, the favorable temperature for the nucleation of the phase is ~655 ^{o}C which, is close to the temperature rise at 3044SS side. Lee *et al* have shown the formation of Al_4Fe containing Cr, Ni and Mn within the reaction zone for FSW joint between A6056-T4 Al alloy and 304SS [21]. However this phase is perhaps metastable in nature and in the phase diagram the presence of the same has not been indicated. Friction welded joint between 6061-T6 aluminium alloy and 304SS has also indicated the formation of Fe_2Al_5 in the reaction zone [20]. The occurrence of FeAl, Fe_3Al and Fe_2Al_5 has been also explored by Fukumoto and his co-workers for welded joints consisting of 1050Al and 304SS under different conditions [22]. Variable size Fe rich particles are found within the SZ of aluminium matrix owing to tool rotation, as it removes material from butting edge of 304SS and broken particles are deposited in Al matrix. The selected area diffraction pattern confirms these particles as ferrite. Austenite to ferrite transformation is driven by induced strain [21]. Strain generation during processing is evident with the formation of highly dense dislocation sub-structure having small aspect ratio within the Al matrix. This observation was also illustrated by Oertelt *et al* for FSW of 2195 Al alloy and Lee *et al* for FSW of 6005 Al alloy [21, 23]. Severe plastic deformation at an elevated temperature clearly indicates recrystallization at SZ during friction stir welding by dynamic process.

Within the thermo-mechanically affected zone, severity of plastic strain decreases. The phenomenon is endorsed by the decrement of dislocation density, increment in cell aspect ratio and increment in grain size of substrate with respect to the SZ. Recrystallization is absent in this region. HAZ does not have significant microstructural change with respect to base metal (BM); the only difference is less dislocation density in HAZ with respect to the latter owing to heat conduction through the zone. This indicates thermal softening in HAZ. Failure under tensile loading occurred in ductile mode. Fracture took place primarily through the stirring zone of aluminum substrate; however, in some location it interacts with the intermetallic phase. The reaction zone resembles with composite microstructure as the intermetallics are dispersed within the matrix of aluminium. The inherent brittleness of the intermetallics lowers the bond strength of the CP Al to 304SS FSW joint. The intermetallic compound also restricts the material flow during tensile testing by their pinning action; hence the ductility of the joint is poor with respect to the substrate. Fracture location also shows, that the weakest region of this dissimilar assembly lies within the reaction zone.

Conclusions

Commercially pure aluminium has been successfully joined with 304 stainless steel by friction stir welding. Microstructural study and evaluation of mechanical properties of the assembly reveal the followings:

1. Melting point and the strength of 304SS is higher than the CP Al; hence tool rotation occurred mainly within the aluminum side.
2. SEM with EDS observation indicates limited diffusion of aluminum within 304SS. On the other hand, within the diffusion zone of CP Al substantial quantity of Fe, Cr and Ni are present.
3. Structural change mainly occurred within the CP Al side. These zones are characterized by different grain size and dislocation density owing to temperature and extent of deformation gradient.
4. Inter-diffusion of chemical species across the bondline leads to form discrete islands of Fe_3Al intermetallic phase within the diffusion zone.
5. Rubbing action of tool over the butting edge results in removing fine particles of 304SS and they got embedded in the SZ of Al matrix. At the latter stage austenite underwent phase transformation to ferrite.
6. Fracture path mainly moves through SZ of Al alloy under tensile loading; however in some places presence of Fe_3Al compound has been also observed.

Acknowledgement

The authors wish to thank Prof. S.P. Mehrotra, Director, National Metallurgical Laboratory and Dr. R. N. Ghosh, Sr. Dy. Director and Head-MST Division, National Metallurgical Laboratory for their continuous inspiration to carry out the investigation and kindly permitting to publish this work. The authors also acknowledge the partial financial support from DST, Govt. of India to carry out the investigation.

References

1. W. M. Thomas, E. D. Nicholas, J. C. Needham, M. G. Murch, P. Temple-Smith and C. J. Dawes: Int. Patent Appl. No. PCT/GB92/02203.
2. J. H. Cho, D. E. Boyce and P. R. Dawson, *Mats Sci & Engg A*, 358 (2005 146-163.
3. T. R. McNelley, S. Swaminathan and J. Q. Su, *Scripta. Mater.,* 58 (2008) 349-354.
4. S. A. Khodir, T. Shibayanagi and M. Naka*, Materials. Trans.*, 47 (2006) 185-193.
5. H. S. Park, T. Kimura, T. Murakami, Y. Nagano, K. Nakata and M. Ushio, *Mats. Sci. Engg A*, 371 (2004) 160-169.
6. S. H. C. Park, Y. S. Sato and H. Kokawa, *Scripta. Mater.*, 49 (2003) 161-166.
7. M. B. Prime, T. G. Herold, J. A. Baumann, R. J. Lederich, D. M. Bowden and R. J. Sebring, *Acta. Mater.,* 54 (2006) 4013-4021.
8. I. Shigematsu, Y. J. Kwon, K. Suzuki, T. Imai and N. Saito, *J. Mats. Sci. Letts.*, 22 (2003) 353-356.
9. W. B. Lee, Y. M. Yeon and S. B. Jung: *J Mats. Sci., 38* (2003) 4183-4194.
10. J. A. Wert, *Scripta. Mater.*, 49 (2003) 603-612.
11. W. M. Thomas, P. L. Threadgill and E. D. Nicholas, *Sci. Technol. Weld J.*, 4 (1999) 365-372.
12. T. J. Lienert, W. L. Stellwag, B. B. Grimmett and R. W. Warke, *Weld J.*, 82 (2003) 1s-9s.
13. A. P. Reynolds, W. Tang, M. Posada and J. DeLoach, *J. Sci. Technol. Weld. J.*, 8 (2003) 455-460.
14. H. Fujii, R. Ueji, Y. Takada, H. Kitahara, N. Tsuji, K. Nakata and K. Nogi, *Mater. Trans.*, 47 (2006) 239-242.
15. Y. S. Sato, T. W. Nelson, C. J. Sterling, R. J. Steel and C. O. Pettersson, *Mats. Sci. Engg. A*, 397 (2005) 376-384.
16. P. Miao, G. R. Odette, J. Gould, J. Bernath, R. Miller, M. Alinger and C. Zanis, *J. Nuclear Mats.*, 367-370 (2007) 1197-1202.
17. P.L. Menezes: Ph.D Thesis, *Role of surface texture on friction and transfer layer formation – a study using pin-on-plate sliding tester*, IISc Bangalore (India), August 2007, p.148.
18. K. Kumar and S. V. Kailas, *Mats. Sci. and Engg. A*, 485 (2008) 367-374.
19. K. Kumar and S. V. Kailas, An insight into understanding the intrinsic mechanisms governing the formation of friction stir welds in joining of metals. In Proc. of *Sixteenth International Conference on Processing and Fabrication of Advanced Materials, Singapore*, Dec'2007, pp. 341-356.
20. T. Yokoyama, *Materials Sci. Technol.*, 19 (2003) 1418-1426.
21. W. B. Lee, M. Schmuecker, U. A. Mercardo, G. Biallas and S. B. Jung, *Scripta Mater.*, 55 (2006) 355-358.
22. S. Fukumoto, H. Tsubakino, K. Pkita, M. Aritoshi and T. Tomita, *Mater. Sci. Technol.*, 14 (1998) 1080-1086.
23. G. Oertelt, S. S. Babu, S. A. David and E. A. Kenik, *Welding Res. Suppl.*, March'2001, pp. 71s-79s.